Chapter 9
Reduced Order Model Efficiency for Structural Health Monitoring using Modal Data: A Case Study of Milad Tower

Akbar Esfandiari, Maryam Vahedi, Saeed Behboodi, and Masoud Sanayei

Abstract There are many methods for parameter estimation and damage detection of ordinary structures. However, for high-rise and massive structures where extraction of higher mode shapes and higher-frequency structural responses, which are more sensitive to structural variation, are challenging, the available indices such as MAC or COMAC may not work. Hence, this research presents a modified form of COMAC indices through weighting for structural health monitoring of Milad Tower, as a case study of a high-rise structure. A reduced-order model of the Milad Tower is used instead of the full finite element model. The capabilities of the different parameter estimation methods for model updating and damage assessment are investigated. The effectiveness of the proposed method is evaluated using numerically simulated data that demonstrates acceptable levels of accuracy and reliability in detecting, locating, and quantifying structural damages. Additionally, unavoidable challenges such as incomplete measurements of structural responses, modeling errors, and measurement errors are investigated. Also, the measured structural responses are used to assess the behavior of the proposed indices. The reduced-order model's efficiency and the proposed method's practical applicability using the new indices are demonstrated. The proposed weighted form of the COMAC index is more sensitive to changes in structural parameters. In addition, a model updating algorithm is proposed for damage detection using the new reduced-order model based on the consistent mass matrix. The proposed method was successfully applied to the Milad Tower using modal data. It resulted in a more accurate reduced-order model for damage detection.

Keywords Towers · Reduced finite element model · Modeling error · Modeling efficiency · Computational efficiency · Modal data

Introduction

In structural model updating for health monitoring procedures, utilizing a full-scale three-dimensional finite element model of a high-rise structure provides a massive amount of data, which may result in errors in data collection. In addition, the data analysis of large-scale structures using the full-scale model could be prohibitive in terms of modeling time and computation time. In this regard, developing a lower-dimensional model that accurately captures the characteristics of the original model in the frequency range of interest would be beneficial. Generating a reduced Finite Element model is based on selecting the desired number of Degrees of Freedom (DOFs), which results in reduced-order mass, damping, and stiffness matrices [1].

Akbar Esfandiari
Associate Professor, Amirkabir University of Technology, Department of Maritime Engineering, Tehran, Iran
e-mail: a_esfandiari@aut.ac.ir

Maryam Vahedi
Research Associate, Amirkabir University of Technology, Dept. of Civil and Env. Engineering, Tehran, Iran
e-mail: M_vahedi@aut.ac.ir

Saeed Behboodi
Research Assistant, University at Buffalo (SUNY), Dept. of Mechanical and Aerospace Engineering, Buffalo, New York 14260, USA; Former Research Assistant, Amirkabir University of Technology, Dept. of Civil and Environmental Engineering, Tehran, Iran
e-mail: saeed.behboodi@ut.ac.ir

Masoud Sanayei
Professor, Tufts University, Department of Civil and Environmental Engineering, Medford, MA 02155, USA
e-mail: masoud.sanayei@tufts.edu

Matthew Whelan et al. (eds.), *Dynamics of Civil Structures, Vol. 2*, Conference Proceedings
of the Society for Experimental Mechanics Series, https://doi.org/10.13052/97887-438-0147-4_9

Many researchers have addressed the issue of high-rise building monitoring, based on which it can be concluded that dealing with large data and finite element modeling of large-scale real-life structures poses challenges when used in numerical simulations [2–7]. These challenges are magnified in inverse problems and model updating algorithms. Additional specialized scripts are needed to communicate with commercial software for structural health monitoring and interactive communication between commercial software and research software [8]. This way, SHM and model updating of a large structure using different commercial software is time-consuming.

Model order reduction techniques aim to create a simplified model, commonly called a reduced-order model (ROM), based on a large and complex full-scale model (FSM) using commercial software. The approximation errors must be negligible compared to the full-scale FE model in terms of the frequency range of interest and the dynamic properties and characteristics of the complete model. Furthermore, it must be computationally efficient, reliable, and low-cost.

The Guyan condensation method can reduce finite element models using static condensation [9]. Hence, it does not preserve the inertial forces applied to the model. Dynamic condensation methods have been developed to remove the weakness of the Guyan method [10,11]. O'Callahan et al. [11] proposed the system equivalent reduction expansion process (SEREP). This method is introduced as the most accurate method in many studies. Marinone et al. [12] proposed an improved method by combining the SEREP and Guyan methods. Regardless of the existing and challenging problems of the proposed data expansion and model reduction methods, applying these methods to large civil infrastructure is impractical. For structural model updating and conceptual analysis of large structures, it is preferred that the entries of the stiffness matrix are meaningful and that connectivity between the DOFs is preserved. Such a model can be used for sensitivity analysis and investigation of the influence of different parameters on structural responses. The methods above may not preserve the connectivity of elements for model reduction. Furthermore, the transformation matrix for model reduction shall be updated at each iteration.

Large models can be simplified at the substructure level based on the available condensation techniques [13]. This approach preserves the connectivity between the master DOFs. Many researchers frequently use the Guyan static condensation and dynamic condensation methods. Comprehensive studies on these methods were conducted by Allen et al. [14] and Qu [15]. However, these methods require unavailable details of stiffness and mass matrices as inputs, limiting their application to large structures modeled by commercial software.

Wu and Li [16] updated a simple finite element model of the 310 m tall Nanjing TV Tower based on ambient vibration measurements. The FE model consisted of 17 beam elements and lumped masses. The tapered beam elements used by Cheng [17] were replaced by equivalent piece-wise uniform prismatic beams, and lumped masses were assumed.

The simplified models of large civil structures are based on fundamental principles and definitions of structural behavior. Yi et al. [18] extracted the lumped mass matrix and entries of the stiffness matrix of the Dalian World Trade Center's building. The simplified model was used to study the optimal sensor placement on the building. Ni et al. [19] proposed a reduced model for structural health monitoring of the Canton Tower. They assigned six active DOFs at each defined level. The stiffness matrix was extracted sequentially by applying unit loads at active DOFs one at a time. The mass matrix was extracted as a lumped mass. Only the reduced model's stiffness parameters were tuned to remove the observed discrepancy between the full-scale and the reduced model. The ROM was used in other studies focused on structural health monitoring and structural identification of the Canton Tower [20, 21]. The difference between the modal properties of the reduced and full-scale models was increased due to inaccurate mass modeling.

Xiong et al. [22] proposed a reduced model for the Shanghai Tower, a 125-story, 632-meter building. The stiffness matrix was extracted by applying unit displacement at the defined DOFs at the interfaces of individual zones, and further steps extracted the lumped mass matrix. The mass and stiffness matrix of the ROM was calibrated to match the extracted model data by the full-scale model.

The lumped mass matrix is a source of modeling error that adversely affects the model characteristics and, consequently, model updating accuracy. Coarse meshing further increases induced modeling errors by a lumped mass matrix. It must be emphasized that reducing modeling errors is an essential task for structural model updating.

In this research, a novel method is proposed to extract the consistent mass matrix of a large tower. The algorithm is based on the extracted data from the structure's full-scale finite element model. Then, the proposed reduced-order model based on the reduced consistent mass matrix model is verified by comparing the dynamic characteristics of the tower's ROM versus the FSM. A new form of the Coordinate Modal Assurance Criterion (COMAC) index is proposed by appropriate weighting (normalization) of the mode shapes. The proposed weighted form of the COMAC index is more sensitive to changes in structural parameters. The mass matrix of the obtained ROM is then updated to be utilized for damage detection. In addition, a model updating algorithm is proposed for damage detection using the new reduced-order model based on the consistent mass matrix. The proposed method was successfully applied to the Milad Tower using modal data. It resulted in a more accurate reduced-order model for damage detection.

Research Methodology

a. General overview of the Milad Tower

Milad Tower, also known as Tehran Tower, is a multi-purpose tower in Tehran, Iran. It consists of five main parts: the foundation, the lobby, the main body of the tower (shaft), the head structure (basket), and an antenna mast with a length of 120 meters. Tower construction started in 1997, and it opened on October 7, 2008.

The main shaft, rising through the middle of the main lobby, transmits loads from the upper parts of the tower, such as the head and antenna, to the foundation. It is a concrete structure that extends from the ground level to 315 meters.

The head structure of the tower is a 12-story building that includes a variety of utilities, including telecommunication floors, shops, a restaurant, and an observation deck. The head structure weight is about 2,000 tons and is attached to the tower's main body from the level of 247 to 308 meters. The minimum diameter of the head structure is 25 meters, and the maximum diameter is 60 meters. The last part of the Milad Tower is the antenna structure made of pure steel with a length of 120 meters and an approximate weight of 350 tons. The total weight of the Milad Tower, including the shaft, head, and antenna, is about 150,000 tons. A schematic of the tower's elevations and plan sections of the concrete core is illustrated in Figure 1.

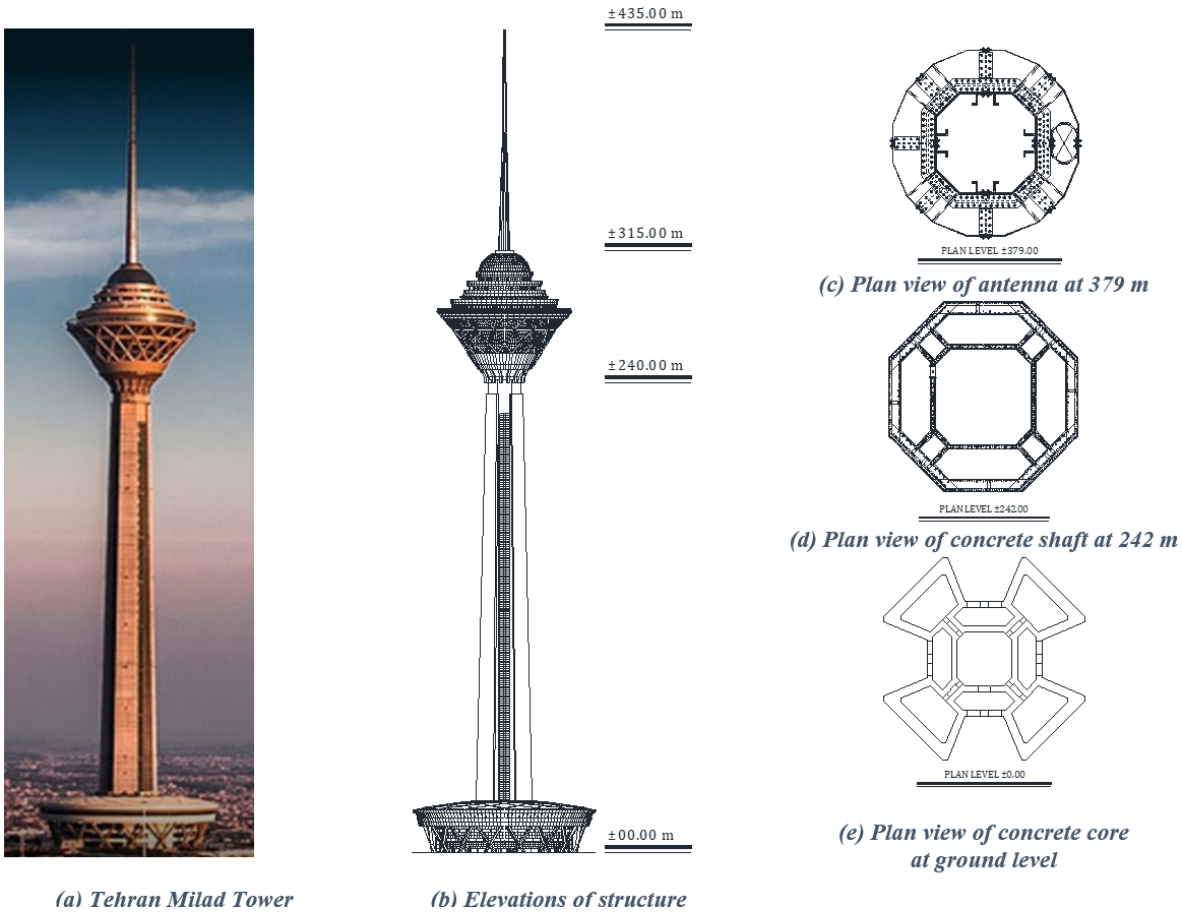

Fig. 1 Elevations of Milad Tower and plan sections of concrete core at various levels.

b. Full-scale model of the Milad Tower

The full-scale 3D finite element model of the Milad Tower was primarily developed as a baseline model based on design drawings of the Tower. This FSM, which consists of 4,495 frame elements, 18,489 shell elements, 17,850 nodes, and 106,524 degrees of freedom, was created in the SAP2000 commercial finite element analysis software. The main part of the Milad Tower structure is the concrete shaft modeled with shell elements. The head structure is a 12-story steel structure modeled

as a space frame with additional floor elements. The loads are transferred from floors to beams and columns to the shaft. The natural and mode shapes of Milad Tower are shown in Figure 2.

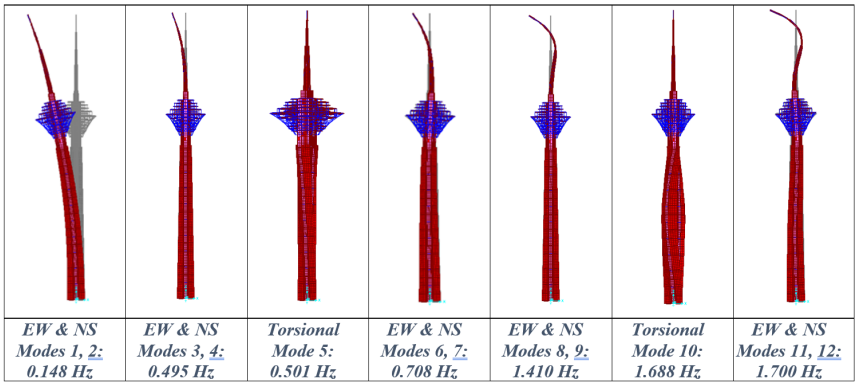

Fig. 2 Milad Tower modes of vibrations obtained from finite element FSM.

The natural frequencies of the first 12 modes were below 1.7 Hz. Modes 1 and 2 are the tower/antenna repeated bending modes about the principal axes. Whereas modes 3,4, and 6, 7, as well as 8, 9, and 11, 12 represent four pairs of repeated modes. Modes 5 and 10 are the torsional modes of the tower.

c. 3D Reduced-Order Model

The proposed method for estimating the reduced consistent mass matrix is a general method that can be applied to different types of structures. However, the method is discussed in detail based on the geometry and mechanical properties of the Milad Tower to develop the stiffnesses and mass super-elements for each segment of the structure. To create the ROM, the FSM is discretized and reduced into 34 super-elements along the shaft's centroidal axis for modeling axial, shear, and bending behaviors. The elements' end node selection was dependent on the floor slab levels in the shaft and the desired sensor locations for future structural health monitoring.

The ROM's first 20 elements are related to the shaft (height of 0 to 248.5 m), element 21 corresponds to the head structure (height of 248.5 to 302.4 m), and the last 13 elements represent the antenna structure (height of 302.4 to 435.55 m). Therefore, the overall reduced-order model includes 34 elements with 204 degrees of freedom.

Extraction of the stiffness matrix: For each element of the ROM, a unit displacement must be applied to each defined 12 degrees of freedom one at a time while the rest of the DOFs are constrained. The magnitude of the force required at each active DOF represents the column of the stiffness matrix corresponding to the active DOF. However, using any commercial software, this procedure could be performed by applying a unit force at the active DOF, constraining all other master DOFs, and obtaining the resisting forces. Then, the obtained values of the resisting forces shall be magnified to achieve a unit displacement. A schematic of the applied unit displacement is presented in Figure 3. Repeating the above procedure for each of the 34 super-elements will result in stiffness matrices at the element level that are assembled to form the global stiffness matrix of the ROM.

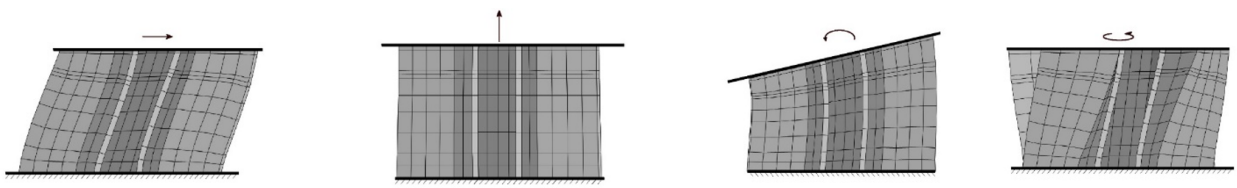

Fig. 3 Unit translation or rotation (force or moment) imposed at different master DOFs of a super-element.

Extraction of the reduced lumped mass matrix (RLMM): While extracting the stiffness matrix of a ROM based on commercial software is straightforward, extracting the mass matrix is challenging. Hence lumped mass matrices are often used

by reduced-order algorithms. In the RLMM, the total mass of each element is divided directly equally between the translational degrees of freedom for each direction at the adjacent nodes. The rotational entries of the lumped mass matrix are diagonal and defined as Eq. (1):

$$m_r = \sum_{i=1}^{s} l_i^2 m_{ii} \tag{1}$$

where m_{ii} is the translational mass at the ith node and l_i is the distance between node i and the reference (master) node of the reduced model. This formulation depends on the structure's overall geometry and does not present the dominant behavior of the structural elements. A lumped mass matrix introduces modeling errors that can corrupt the model updating process. Additionally, the mass modeling error by the lumped mass method becomes large when using a coarse mesh.

Extraction of the reduced consistent mass matrix (RCMM): The following steps are followed to extract the consistent mass matrix for each super-element.

Step1) Mass at translational and rotational DOFs: A typical super-element of a segment of the full-scale model is shown in Figure 4. A master DOF of this super-element is considered to be active, while all other degrees of freedom are constrained. The master DOF can be translational or rotational to study the lateral modes of vibration.

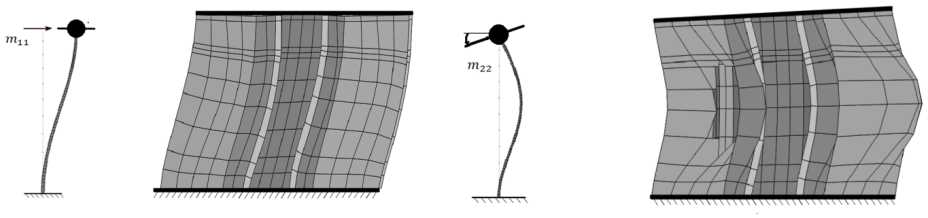

(a) Translational DOF *(b) Rotational DOF*

Fig. 4 A single active DOFs for extraction of a consistent mass matrix of a super-element.

In such cases, the equation of motion of the ROM will be equal to the equation of motion of a single degree of freedom model, and the eigenvalue equation shown in Eq. (2) is used to find the corresponding mass:

$$k_{ii} - {\omega_i}^2 m_{ii} = 0 \tag{2}$$

where k_{ii} is the stiffness at the ith node and ω_i is the ith circular natural frequency. The corresponding stiffness entry k_{ii} was previously estimated during the stiffness extraction process. By using the calculated natural frequency using each segment of the full-scale model, the corresponding diagonal entries of the ROM mass matrix can be calculated by Eq. (3):

$$m_{ii} = \frac{k_{ii}}{{\omega_i}^2} \tag{3}$$

This step must be repeated for translational and rotational DOFs of each super-element of the FSM for calculation of the ROM for each element.

Step2) Mass coupling of a translational and a rotational DOF: While transverse and rotational deformations are uncoupled from both axial and torsional deformations in a bi-symmetrical section, the transverse and rotational DOFs are coupled together. To extract the off-diagonal entries of the ROM mass matrix in a 3D space, both coupled DOFs must be active simultaneously while the other 10 DOFs are constrained. A schematic representation of such a case is given in Figure 5 for the extraction of off-diagonal entries of the consistent mass matrix.

The circular natural frequencies of the two DOF models are expressed by the corresponding eigenvalue equation in Eq. (4):

$$\det\left(\begin{bmatrix} k_{ii} & k_{ij} \\ k_{ij} & k_{jj} \end{bmatrix} - {\omega_{ij}}^2 \begin{bmatrix} m_{ii} & m_{ij} \\ m_{ij} & m_{jj} \end{bmatrix} \right) = 0 \tag{4}$$

where i and j are active DOFs of a segment of the structure and ω_{ij} is the circular natural frequency of the constrained segment that is evaluated using the FSM. Note that the corresponding stiffness matrix is already estimated in the previous steps. Hence, the only unknown term is the off-diagonal mass entry m_{ij} due to the coupling of the horizontal and rotational DOFs is calculated using Eq. (4). This procedure must be repeated for all off-diagonal entries of the mass matrix ($m_{2,4}$,$m_{1,5}, m_{5,7}, m_{4,8}, m_{8,10}, m_{7,11}, m_{1,11}, m_{2,10}$).

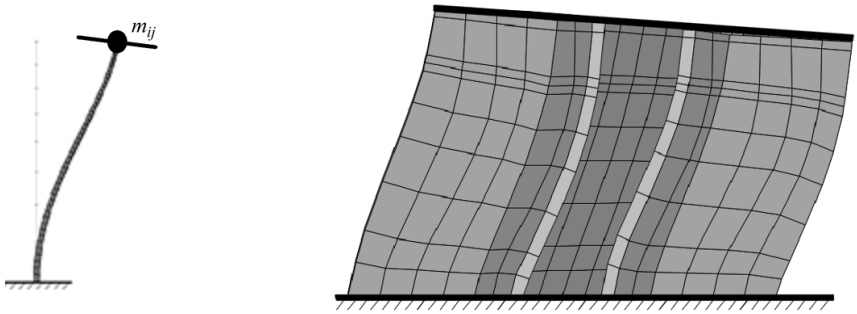

Fig. 5 Simultaneous activation of two coupled DOFs (transverse & rotational).

According to the structural stability concepts, two transverse DOFs of a single segment cannot be defined as active simultaneously. Hence, to extract such an off-diagonal mass entry, two segments of the model must be considered simultaneously for computing Eq. (4).

Torsional stiffness: Since the estimation of the torsional modes is frequently imprecise and model updating should be avoided, an alternative technique is proposed for calculating the corresponding torsional entry in the stiffness matrix. For this purpose, the fundamental definition of torsional stiffness has been implemented. A torsional moment T applied at the free end of the model causes a twisting deformation θ. Then the magnitude of the torsional stiffness can be evaluated by Eq. (5):

$$K_t = \frac{T}{\theta} \tag{5}$$

The above technique can be applied at all defined levels to obtain the stiffness matrix entries corresponding to all torsional DOFs of each segment.

Milad Tower Reduced-Order Model Verifications

The ROM must maintain not only the static behavior but also the dynamic behavior of the original FSM. For this purpose, the dynamic characteristics of the ROM are compared with the FSM, including natural frequencies and mode shapes. The natural frequencies of the ROM modal analysis for the first ten lateral modes in the x-direction are presented in Table 2. The lateral mode shapes of the x and y directions are identical due to symmetry. The modal mass ratios were more than 90 percent using these mode shapes. A comparison of the natural frequencies in Table 1 demonstrates the accuracy of the predicted natural frequencies by the ROM based on the reduced consistent mass matrix model compared to the FSM. Additionally, the reduced lumped mass matrix (RLMM) and the reduced consistent matrix (RCMM) models are compared to the FSM. The relative difference of RLMM and RCMM w.r.t. FSM is shown in Table 1. Clearly, the RCMM-based model has outperformed the RLMM-based model based on the calculated natural frequencies.

Table 1 Comparison of natural frequencies of first 10 lateral modes

Mode No.	1	2	3	4	5	6	7	8	9	10
FSM (Hz)	0.148	0.495	0.709	1.41	1.695	2.844	3.128	4.346	4.701	4.767
RLMM (Hz)	0.146	0.514	0.655	1.392	1.519	2.555	2.675	3.683	4.662	5.100
RCMM (Hz)	0.150	0.507	0.742	1.456	1.782	2.828	3.21	4.112	4.726	5.405
% Difference of RLMM w.r.t. FSM	-0.013	0.039	-0.076	-0.013	-0.104	-0.102	-0.145	-0.153	-0.008	0.070
% Difference of RCMM w.r.t. FSM	0.014	0.024	0.047	0.033	0.051	-0.006	0.026	-0.054	0.005	0.134

Additionally, to further assess the accuracy of the mode shapes obtained from the FSM and ROM, the first ten lateral mode shapes are shown in Figure 6. It must be mentioned that the mode shapes demonstrated as solid lines are related to the

updated model of RCMM, and the detailed process of updating is stated in the next section. The mode shapes are normalized for comparison based on the corresponding vector size. Since the lateral modes in the x and y-directions are similar, only the x-direction is presented in Figure 6. As shown, the predicted mode shapes by the ROM are very accurate and represent the real behavior of the model using a few elements, considering that the random loads (e.g., wind and earthquake) mainly excite the lower modes. The mode shapes of the updated models based on the RCMM, labeled "Updated RCMM", will be discussed later.

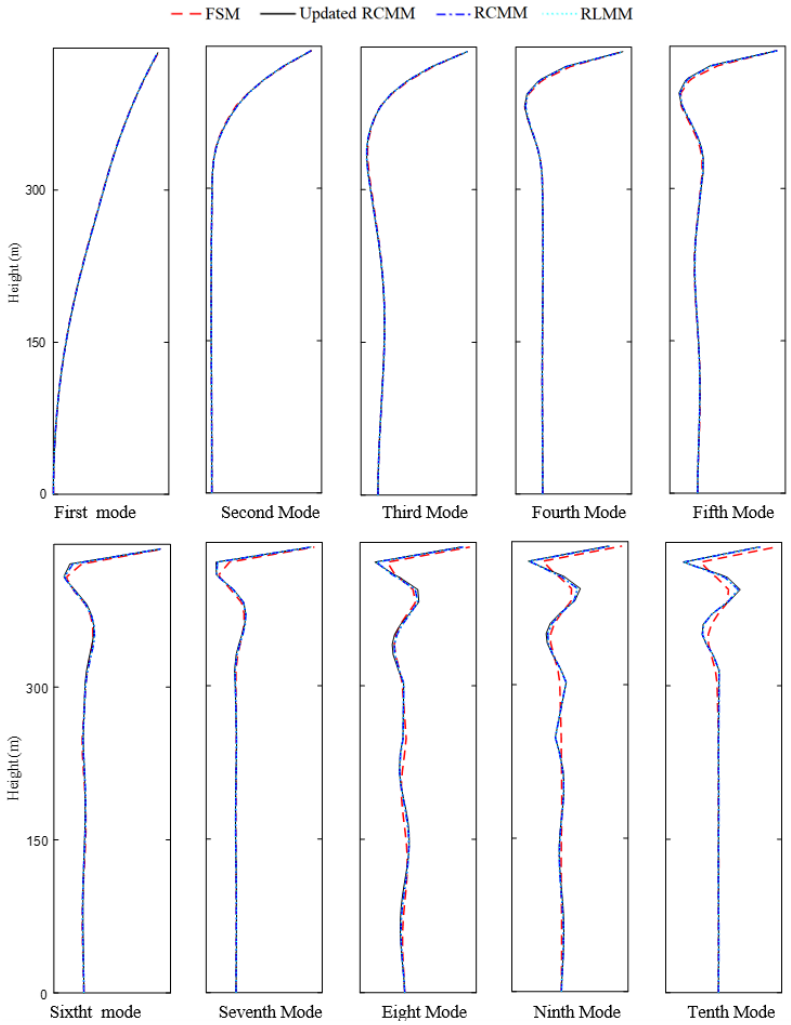

Fig. 6 Comparison of RCMM-based ROM with FSM using first 10 lateral mode shapes.

To conduct a more comprehensive study, the predicted mode shapes by the FSM and both ROMs (RLMM and RCMM) are compared based on the Modal Assurance Criterion (MAC) index defined by Eq. (6) as:

$$MAC\,(i,j) = \frac{\left\| (\phi_{ROM})_j^* (\phi_{FSM})_i \right\|^2}{\left\| (\phi_{FSM})_i^* (\phi_{FSM})_i \right\| \left\| (\phi_{ROM})_j^* (\phi_{ROM})_j \right\|} \tag{6}$$

Where $(\phi_{FSM})_i$, $(\phi_{ROM})_i$, are the ith mode shapes of the full-scale and ROM models, respectively, and the superscript * denotes the transpose complex conjugate of the ith mode shape. Table 2 gives the calculated values.

The MAC values in Table 2 indicate that the predicted mode shapes for the FSM and ROM based RCMM are very consistent. It also shows that the presented RCMM model is more accurate than RLMM.

Table 2 Comparison of RLMM & RCMM-based ROMs with FSM using MAC values of different mode shapes

Index	Model	Mode No.									
		1	**2**	**3**	**4**	**5**	**6**	**7**	**8**	**9**	**10**
MAC	**RLMM**	1.000	1.000	0.971	0.990	0.985	0.867	0.866	0.437	0.156	0.025
	RCMM	1.000	1.000	0.999	0.997	0.991	0.986	0.974	0.947	0.897	0.799

Table 3 Comparison of RLMM & RCMM-based ROMs with FSM using COMAC values of mode shapes at different nodes

DOF (Node No.)	RLMM	RCMM	DOF (Node No.)	RLMM	RCMM
1	0.587	0.979	18	0.618	0.923
2	0.531	0.964	19	0.301	0.816
3	0.520	0.958	20	0.475	0.997
4	0.478	0.939	21	0.760	0.980
5	0.405	0.904	22	0.855	0.962
6	0.280	0.837	23	0.934	0.987
7	0.112	0.748	24	0.931	0.994
8	0.343	0.995	25	0.889	0.964
9	0.642	0.947	26	0.802	0.919
10	0.681	0.998	27	0.659	0.925
11	0.503	0.964	28	0.775	0.990
12	0.352	0.886	29	0.825	0.993
13	0.186	0.774	30	0.819	0.943
14	0.322	0.952	31	0.599	0.982
15	0.695	0.904	32	0.844	0.971
16	0.763	0.973	33	0.828	0.909
17	0.824	0.988	34	0.811	0.991

To compare the accuracy of different models locally, the Coordinate Modal Assurance Criterion (COMAC) index is defined by Eq. (7), where i is the node number and L is the number of mode shapes.

$$COMAC\,(i) = \frac{\int_{l=1}^{L} \left|(\phi_{FSM})_{il}(\phi_{ROM})_{il}^{*}\right|2}{\int_{l=1}^{L} (\phi_{FSM})_{il}^{2} \int_{l=1}^{L} (\phi_{ROM})_{il}^{2}} \tag{7}$$

The COMAC values at 34 nodes of the structure are shown in Table 3, which indicates the precision of the RCMM. The COMAC values show the deformation at a specific level obtained by the full-scale and reduced-order models for different mode shapes that are close. COMAC index values closer to 1.0 indicate higher accuracies at a DOF.

It must be emphasized that a coarse mesh might not be able to represent the structural behavior at higher modes, and a finer mesh is required. Hence, it is expected that the MAC values at the higher modes will be less than those at the lower modes. Also, COMAC values are sensitive to the local behavior of the structure. More points are required to capture the real behavior in the higher curvature regions. Hence, the discrepancy between ROMs and FSM can increase in such regions.

Model Updating and Damage Detection

a. Weighted-COMAC damage index

The Modal Assurance criterion (MAC) and the Coordinate Modal Assurance Criterion (COMAC) are widely used for structural damage detection and model validation. For a large structure like Milad Tower, the sensitivity of these indices with respect to variation of structural parameters is the main issue. In such cases, the variation of indices due to structural damages might be overshadowed by the variation of indices due to measurement errors. The COMAC index values depend on the technique selected for normalization (Weighting) of the mode shapes. The partially measured mode shape is scaled (weighted) by its second norm as a practical choice. Although there is no difference between the MAC values for the arbitrary scaled or mass-normalized mode shapes, the values for COMAC are quite different. The values of COMAC indices

using normalized mode shapes and error-contaminated data are compared with the exact values in Figure 7. It is reminded that the COMAC values for the intact model without errors are equal to 1.0.

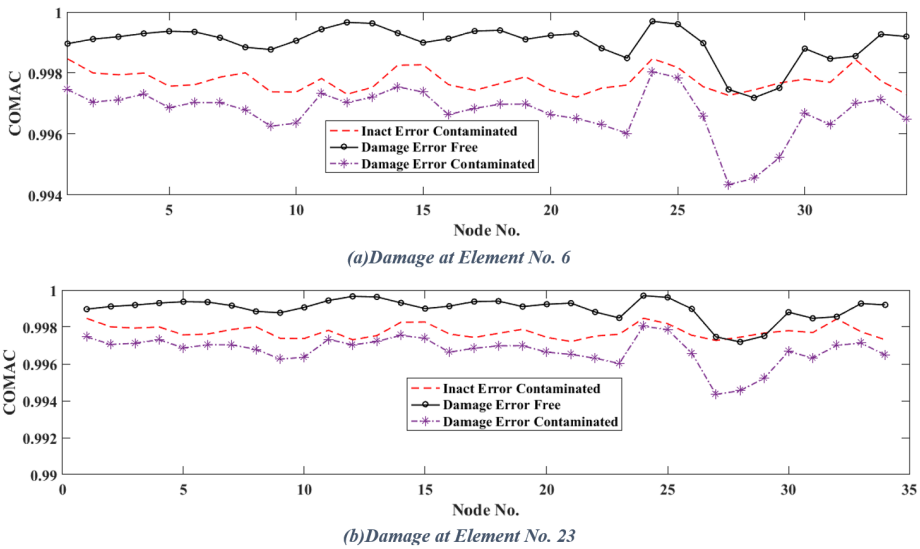

(a)Damage at Element No. 6

(b)Damage at Element No. 23

Fig. 7 COMAC values for different cases with 10 percent of stiffness variations (Normalized by 2^{nd} norm).

Figure 7 shows that COMAC indices are highly sensitive to measurement errors, which might overshadow their sensitivity to stiffness variations. This may cause errors in a damage detection process. To provide the ability to observe more changes in COMAC index values due to damage and less sensitivity to measurement errors, arbitrary scaled mode shapes are used to calculate the COMAC values. For this purpose, the mode shape value at a specific node is considered for mode shape normalization, resulting in the weighted-COMAC index values.

Figure 8 shows the weighted-COMAC index values for normalized mode shapes with respect to the mode shape value at node 10. It is notable that the weighted-COMAC values of the error-contaminated damaged and intact models are very close to each other. As shown below, using the weighted-COMAC index values provides excellent observability of damage with less sensitivity to measurement errors.

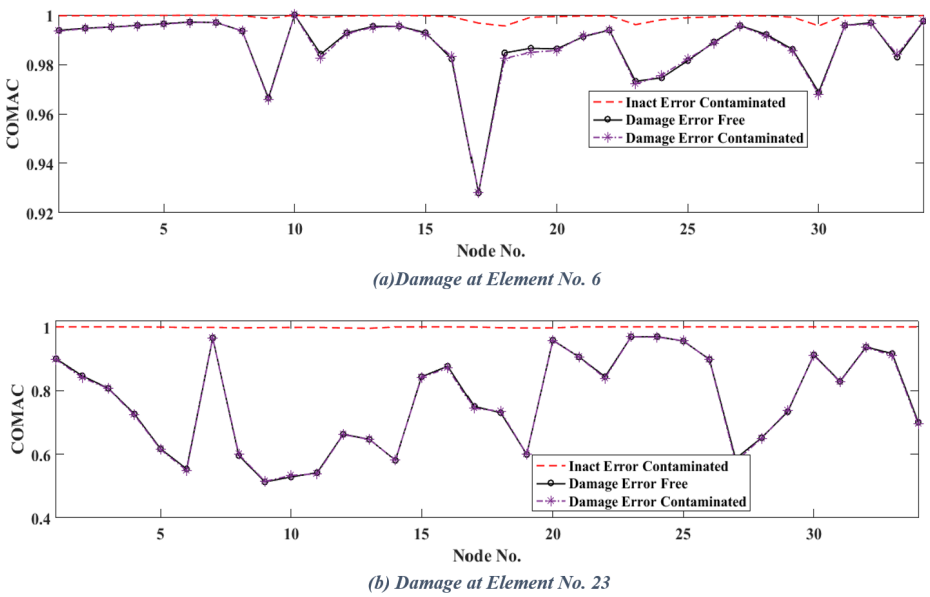

(a)Damage at Element No. 6

(b) Damage at Element No. 23

Fig. 8 Weighted-COMAC values for different cases with 10 percent of stiffness variations (Normalized by node 10).

b. Model updating algorithm

Although the focus of this paper is on presenting a ROM for general purposes, the ROM might be used for structural model updating and damage detection. Hence, the presented ROM based on the consistent mass matrix is used for structural model updating. The proposed RCMM model is accurate enough for structural response evaluation and conceptual analysis. However, a more accurate reduced model might be essential for structural model updating and damage detection. Hence, the ROM can be tuned through a model parameter estimation process. Since the extraction of the stiffness matrix is based on the static response and is straightforward, in this study, the extracted reduced consistent mass matrix is tuned for a better match of the modal data of the ROM and the full-scale model.

For an n degree of freedom structure, the eigenvalue equation is expressed as:

$$\left(\boldsymbol{K}-\omega_i^2\boldsymbol{M}\right)\phi_{\boldsymbol{i}}=0 \tag{8}$$

where $\boldsymbol{K}$ and $\boldsymbol{M}$ are $(n\times n)$ stiffness and mass matrices of the structure, respectively; ω_i is the ith circular natural frequency, and $\phi_{\boldsymbol{i}}$ is the corresponding mode shape (eigenvector) of the structure. Assuming that structural damage causes changes in the stiffness and mass matrices by the amount of $\boldsymbol{\delta K}$ and $\boldsymbol{\delta M}$, the eigenvalue equation for the damaged structure is rewritten as:

$$\left(\boldsymbol{K}+\boldsymbol{\delta K}-\omega_{id}^2(\boldsymbol{M}+\boldsymbol{\delta M})\right)\phi_{\boldsymbol{id}}=0 \tag{9}$$

where the subscript "d" indicates that the variable in equation is associated to the damaged states. Rearranging Eq. (10) yields:

$$\phi_{\boldsymbol{id}}=-\left[\boldsymbol{K}-\omega_{id}^2\boldsymbol{M}\right]^{-1}\boldsymbol{\delta K}\phi_{\boldsymbol{id}}+\omega_{id}^2\left[\boldsymbol{K}-\omega_{id}^2\boldsymbol{M}\right]^{-1}\boldsymbol{\delta M}\phi_{\boldsymbol{id}} \tag{10}$$

Eq. (11) evaluates the ith mode shape of the damaged structure as a function of the changes in mass and stiffness parameters. However, this equation requires the measured mode shapes of the damaged structure. The complete response measurements at all DOFs requires an extensive sensor network, which is impractical. Furthermore, some degrees of freedom embedded within the structure's body are inaccessible for sensor installations. To establish Eq. (10), we approximated the mode shapes of the damaged structure on the right-hand side by the corresponding mode shapes of the intact structure. Then we updated it through an iterative model updating process.

The stiffness and mass matrix of the intact model is the sum of the stiffness matrices of all individual elements:

$$\boldsymbol{\delta K}=\sum_{r}^{n_E}\delta k_r\boldsymbol{K}_r\quad and\quad \delta\boldsymbol{M}=\sum_{r}^{n_E}\delta m_r\boldsymbol{M}_r \tag{11}$$

Where $\boldsymbol{K}_r$ and $\boldsymbol{M}_r$ are the respective contributions of the rth element to the global stiffness and mass matrices of the structure and $\boldsymbol{n}_E$is the number of elements. The scalar multiplier δk_r and δm_r present the proportional changes in the stiffness and mass of the rth element in the damaged state from their values in the intact state. Substituting (11) in (10), the ith mode shape of the damaged structure can be related to the changes of stiffness and mass parameters as:

$$\phi_{id}=\left[\boldsymbol{S}_{\phi_i}^K\right]\{\delta k\}+\left[\boldsymbol{S}_{\phi_i}^M\right]\{\delta m\} \tag{12}$$

where, rth columns of the sensitivity matrices $\boldsymbol{S}_{\phi_i}^K$and $\boldsymbol{S}_{\phi_i}^M$, which expresses the relation of the ith mode shape at all degrees of freedom to the change of rth stiffness and mass parameter, are evaluated as:

$$\begin{aligned}\boldsymbol{S}_{\phi_i}^K(:,r)&=-\left[\boldsymbol{K}-\omega_{id}^2\boldsymbol{M}\right]^{-1}\boldsymbol{K}_r\phi_i\\ \boldsymbol{S}_{\phi_i}^M(:,r)&=+\omega_{id}^2\left[\boldsymbol{K}-\omega_{id}^2\boldsymbol{M}\right]^{-1}\boldsymbol{M}_r\phi_i\end{aligned} \tag{13}$$

The proposed method extracts the mass matrix of each super-element. Hence, any entries of the RCMM can be the subject of model calibration which could be a challenging issue. Hence, an unknown parameter is assigned to all entries of the consistent mass matrix and the mass matrices of all defined super-elements are updated. The number of unknown mass parameters is 34. The modal data of the first seven mode shapes of the full model are used as the input data for model updating. The updated mass parameters and comparison of the natural frequencies are given by Figure 9 and Table 4.

As the extracted natural frequencies based on the updated mass matrix show, there is an excellent match between the natural frequencies of the updated RCMM model and the full model. To assess the capabilities of the tuned RCMM model to identify simulated structural damages, the stiffness of the super-element 10 (of the shaft from 84 to 96 m height) is reduced by 30 percent. The modal data are extracted from the FSM and used as the input for model updating based on the introduced parameter estimation method. The predicted damage location and severity are shown in Figure 10.

The predicted structural stiffness parameters demonstrated the superior capabilities of the proposed ROM based on the RCMM for structural model updating and health monitoring.

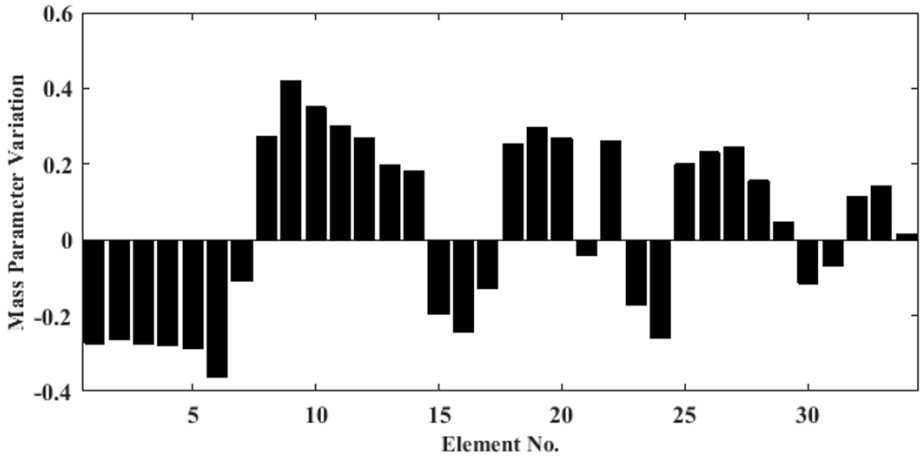

Fig. 9 Updated Mass Parameters of RCMM-based ROM using Mode shape Data.

Table 4 Comparison of Initial and Updated natural frequencies after RCMM mass parameter modification.

Mode No.	FSM	RCMM (Initial)	RCMM (Updated)	Relative Difference w.r.t FSM (%)	
				Initial	Updated
1	0.150	0.148	0.1500	1.214	0.0001
2	0.507	0.495	0.5070	2.511	-0.0016
3	0.742	0.709	0.7416	4.727	0.0560
4	1.456	1.410	1.4560	3.226	-0.0002
5	1.782	1.706	1.7695	5.221	0.7034
6	2.828	2.832	2.8383	-0.514	-0.3651
7	3.210	3.131	3.2060	2.666	0.1238

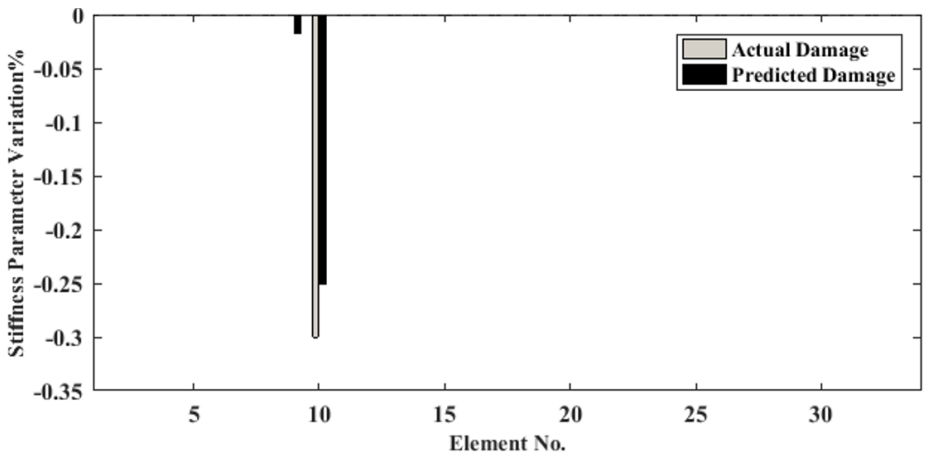

Fig. 10 Updated Stiffness Parameters of RCM-based ROM using Mode shape Data.

Conclusions

Reduced-order models (ROMs) are desired for structural analysis of large structures. These reduced structural models can be used instead of full-scale models (FSMs) for fast computing, conceptual assessment of different models, and model updating for structural health monitoring. ROMs must preserve the inherent properties of FSMs. Unavoidable errors in lumped mass modeling by ROMs may reduce the accuracy of structural responses, leading to magnified errors in model updating methods. In this research, an accurate method for extraction of the ROM of large structures is proposed. Extraction of an accurate mass

matrix for ROMs can be challenging. To reduce modeling errors induced by lumped mass matrices, the reduced consistent mass matrix (RCMM) is extracted based on the evaluated stiffness and natural frequencies of the FSM. The proposed method is applied to the Milad Tower.

The comparison of the predicted structural static and dynamic behavior and modal properties by the proposed ROM (RCMM) demonstrated its ability to reduce large structural models with high accuracy. Additionally, a weighted-COMAC index is proposed, which is more sensitive to structural damage and less sensitive to measurement errors. For damage detection, the updated consistent mass matrix accurately identified the damaged element. Using ROM with RCMM improved modeling accuracy with significant savings in computing time. The proposed ROM with RCMM, in conjunction with the weighted-COMAC index, can be used to investigate structural behavior further and update the structural model for structural health monitoring.

Acknowledgments The authors appreciate the valuable support of the Municipality of Tehran for funding this research through Amirkabir University of Technology (Contract number 1060-1).

References

1. Dorosti, M., Fey, R., Heertjes, M., van de Wal, M. and Nijmeijer, H., 2014. Finite element model reduction and model updating of structures for control. IFAC Proceedings Volumes, 47(3), pp.4517–4522. DOI:10.3182/20140824-6-ZA-1003.01644.
2. Roussel, M., Glisic, B., Lau, J. M., & Fong, C. C. 2014. Long-term monitoring of high-rise buildings connected by link bridges. Journal of Civil Structural Health Monitoring, 4, 57–67.
3. Li, Q.S., Zhi, L.H., Tuan, A.Y., Kao, C.S., Su, S.C. and Wu, C.F., 2011. Dynamic behavior of Taipei 101 Tower: field measurement and numerical analysis. Journal of Structural Engineering, 137(1), pp.143–155. DOI:10.1061/(ASCE)ST.1943-541X.0000264.
4. Kijewski-Correa, T., Kwon, D.K., Kareem, A., Bentz, A., Guo, Y., Bobby, S. and Abdelrazaq, A., 2013. Smart Sync: An integrated real-time structural health monitoring and structural identification system for tall buildings. Journal of Structural Engineering, 139(10), pp.1675–1687. DOI:10.1061/(ASCE)ST.1943-541X.0000560.
5. Gao, F., Zhou, H., Liang, H., Weng, S., Zhu, H., 2020. Structural deformation monitoring and numerical simulation of a supertall building during construction stage. Engineering Structures, 209, 110033, DOI:10.1016/j.engstruct.2019.110033
6. Xiong, H., Xiong, Q., Zhou, B., Abbas, N., Kong, Q., & Yuan, C. 2023. Field vibration evaluation and dynamics estimation of a super high-rise building under typhoon conditions: data-model dual driven. Journal of Civil Structural Health Monitoring, 13(1), 235–249.
7. Glisic, B., Inaudi, D., Lau, J.M. and Fong, C.C., 2013. Ten-year monitoring of high-rise building columns using long-gauge fiber optic sensors. Smart Materials and Structures, 22(5), p.055030. DOI:10.1088/0964-1726/22/5/055030.
8. Sanayei, M., Rohela, P. Automated finite element model updating of full-scale structures with PARameter Identification System (PARIS) Advances in Engineering Software. 67: 99–110. DOI:10.1016/J.Advengsoft.2013.09.002.
9. Guyan, R.J., 1965. Reduction of stiffness and mass matrices. AIAA journal, 3(2), pp.380–380. DOI:10.2514/3.2874
10. Kidder, R.L., 1973. Reduction of structural frequency equations. AIAA journal, 11(6), pp.892–892. DOI:10.2514/3.6852
11. O'Callahan, J. 1989. "A procedure for an improved reduced system (IRS) model." Proc., 7th Int. Modal Analysis Conf., Society for Experimental Mechanics, Bethel, T, 17–21.
12. Marinone, T., Dardeno, T. and Avitabile, P., 2018. Reduced model approximation approach using model updating methodologies. Journal of Engineering Mechanics, 144(3), p.04018005. DOI:10.1061/(ASCE)EM.1943-7889.0001422.
13. Qu, Z.Q. and Selvam, R.P., 2000. Dynamic condensation methods for viscously damped models. In SPIE proceedings series (pp. 1752–1757).
14. Allen, M.S., Rixen, D., Van der Seijs, M., Tiso, P., Abrahamsson, T. and Mayes, R.L., 2020. Substructuring in engineering dynamics. Springer International Publishing.
15. Qu, Z.Q., 2004. Model order reduction techniques with applications in finite element analysis: with applications in finite element analysis. Springer Science & Business Media.
16. Wu, J.R. Li, Q.S. Finite element model updating for a high-rise structure based on ambient vibration measurements, Engineering Structures 26 (2004) 979–990
17. Cheng WR. The analysis of dynamic characteristics of Nanjing TV Tower. Technical Report of Southeast University, 1992.
18. _Yi, T.H., Li, H.N. and Gu, M., 2011. A new method for optimal selection of sensor location on a high-rise building using simplified finite element model. Structural Engineering and Mechanics, 37(6), pp.671–684.
19. Ni, Y.Q., Xia, Y., Lin, W., Chen, W.H. and Ko, J.M., 2012. SHM benchmark for high-rise structures: a reduced-order finite element model and field measurement data. Smart Structures and Systems, 10(4_5), pp.411–426. DOI:10.12989/sss.2012.10.4_5.411
20. Truong, T.C., Cho, S., Yun, C.B. and Sohn, H., 2012. Finite element model updating of Canton Tower using regularization technique. Smart Structures and Systems, 10(4_5), pp.459–470.
21. Lei, Y., Wang, H.F. and Shen, W.A., 2012. Update the finite element model of Canton Tower based on direct matrix updating with incomplete modal data. Smart Structures and Systems, 10(4_5), pp.471–483.
22. Xiong, H.B., Cao, J.X., Zhang, F.L., Ou, X. and Chen, C.J., 2019. Investigation of the SHM-oriented model and dynamic characteristics of a super-tall building. Smart Structures and Systems, 23(3), pp.295–306. DOI:10.12989/sss.2019.23.3.295